Magnetic Field Upscaling and B-Conforming Magnetoquasistatic Multiscale Formulation

Antoine Marteau, Innocent Niyonzima, Gerard Meunier, Janne Ruuskanen, Nicolas Galopin, Paavo Rasilo, Olivier Chadebec

Magnetic Field Upscaling and B-Conforming Magnetoquasistatic Multiscale Formulation

Antoine Marteau[1], Innocent Niyonzima[1], Gérard Meunier[1], Janne Ruuskanen[2], Nicolas Galopin[1], Paavo Rasilo[2] and Olivier Chadebec[1]

[1]Univ. Grenoble Alpes, CNRS, Grenoble INP, G2Elab, F-38000 Grenoble, France
[2]Electrical Engineering Unit, Tampere University, Tampere, Finland

This paper proposes two novel methods for upscaling the macroscopic magnetic field strength from the local solutions of B-conforming magnetoquasistatic multiscale problems. Unlike the volume average method classically used, these methods yield accurate values of the macroscale magnetic field for problems with strong locally-confined eddy currents which enables B-conforming multiscale formulations of eddy currents problems at higher frequencies.

***Index Terms*—Eddy currents, heterogeneous multiscale method, homogenization, nonhomogeneous media**

I. Introduction

MULTISCALE methods have been extensively studied in the electromagnetic community thanks to their easy parallelization and ability to speed up numerical simulations of problems involving heterogeneous materials such as laminated cores, stranded inductors and soft magnetic composites. These methods make possible the simulation of 3D nonlinear eddy currents problems with composite materials, unlike classical methods such as the finite element method (FEM) which are computationally too expensive for these problems.

Multiscale methods generally necessitate computation of macroscopic quantities from finer scale quantities, also called upscaling. Previous works [1] - [3] use B-conforming formulation that necessitate the upscaling of magnetic field strength, which is usually done using the volume average of the finer scale magnetic field h. In the early work from El Feddi et. al. [1], upscaling of magnetic field using volume average is done at very high frequency. In Bottauscio et. al. [2] and Niyonzima et. al. [3], the multiscale solution is validated at low and medium frequencies. But Meunier et. al. [4] warned that the upscaling of the magnetic and the electric fields h and e can unfortunately be non trivial for eddy currents problems. Indeed, a simple volume average of the finescale magnetic field is not compatible with the Maxwell-Ampère law at macroscopic scale in presence of strong locally confined eddy currents. In their paper, the authors proposed that B-conforming formulation should be avoided to prevent upscaling h.

This paper proposes two novel methods for the upscaling of the magnetic field strength that are always valid. These methods only depend on the solutions of the mesoscale problem and the topology of its conducting region. The paper is outlined as follow, Section II recalls the multiscale model for the B-conforming formulation. The proposed upscaling methods are derived in Section III, and the validation on a 2D eddy currents problem is presented in Section IV.

II. Multiscale modeling

Let $\boldsymbol{\sigma}$ and $\boldsymbol{\nu}$ be the electrical conductivity and magnetic reluctivity. We are interested in solving the following Maxwell's equations (1) on an open domain $\Omega \subset \mathbb{R}^d$ in the magnetoquasistatic regime:

$$\operatorname{curl} \boldsymbol{h} = \boldsymbol{j},\ \operatorname{div} \boldsymbol{b} = 0,\ \operatorname{curl} \boldsymbol{e} = -\partial_t \boldsymbol{b},\ \boldsymbol{j} = \boldsymbol{\sigma}\boldsymbol{e},\ \boldsymbol{h} = \boldsymbol{\nu}\boldsymbol{b}, \quad (1)$$

where $\boldsymbol{h}$, $\boldsymbol{b}$, $\boldsymbol{j}$ and $\boldsymbol{e}$ are the magnetic field strength, magnetic flux density, electric current density and electric field, respectively. The conducting domain is denoted by Ω_{c}, and the nonconducting one by $\Omega_{\mathrm{N}} = \Omega \setminus \Omega_{\mathrm{c}}$. The dimension d is 2 or 3.

A. Fine-scale model on periodic geometry

Let us consider a periodic medium denoted by Ω^ϵ included in Ω, that is a tiling obtained by translation of a periodic unit cell $Y = Y_{\mathrm{c}} \cup Y_{\mathrm{N}}$, where Y_{c} and Y_{N} are its conducting and nonconducting regions. Without loss of generality, the cell Y is chosen as a rectangular hexahedron. In this paper, we make the assumption that the conducting region of the cell Y_{c} is simply connected and does not intersect the boundaries of the periodic cell, i.e. $\partial Y \cap Y_{\mathrm{c}} = \emptyset$, which is tantamount to an insulated periodic cell.

We use a usual B-conforming formulation [5]:

$$\begin{cases} \operatorname{curl} \boldsymbol{\nu} \operatorname{curl} \boldsymbol{a} + \boldsymbol{\sigma}\partial_t \boldsymbol{a} = 0 & \text{in } \Omega^\epsilon, \quad (2a) \\ \boldsymbol{a} \times \boldsymbol{n} = \boldsymbol{a} \times \boldsymbol{n} & \text{on } \partial\Omega^\epsilon, \quad (2b) \\ \operatorname{curl} \nu_0 \operatorname{curl} \boldsymbol{a} = \boldsymbol{j}_{\mathrm{s}} & \text{in } \Omega \setminus \Omega^\epsilon, \quad (2c) \\ \boldsymbol{a} \times \boldsymbol{n} = 0 & \text{on } \partial\Omega, \quad (2d) \end{cases}$$

where the modified magnetic vector potentials $\boldsymbol{a}$ verifies $\boldsymbol{b} = \operatorname{curl} \boldsymbol{a}$ and $\boldsymbol{e} = -\partial_t \boldsymbol{a}$, and has to be gauged in non conducting parts of Ω. Here a known current source $\boldsymbol{j}_{\mathrm{s}}$ and magnetic reluctivity of the vacuum $\boldsymbol{\nu}_0$ are assumed in the non homogenized domain $\Omega \setminus \Omega^\epsilon$.

B. The two scale model

In our multiscale approach, the reference problem (1) is replaced by the macroscale problem and many mesoscale problems both governed by equations similar to (2) and solved in an iterative scheme. Mesoscale fields are defined on the periodic cell Y and admit the following decomposition [4]:

$$\begin{aligned} \boldsymbol{h}(\boldsymbol{y}) &= \boldsymbol{H} + \boldsymbol{J} \times \frac{\boldsymbol{y}}{d-1} + \boldsymbol{h}_{\mathrm{c}}(\boldsymbol{y}), \quad \boldsymbol{b}(\boldsymbol{y}) = \boldsymbol{B} + \boldsymbol{b}_{\mathrm{c}}(\boldsymbol{y}), \\ \boldsymbol{e}(\boldsymbol{y}) &= \boldsymbol{E} - \partial_t \boldsymbol{B} \times \frac{\boldsymbol{y}}{d-1} + \boldsymbol{e}_{\mathrm{c}}(\boldsymbol{y}),\ \boldsymbol{j}(\boldsymbol{y}) = \boldsymbol{J} + \boldsymbol{j}_{\mathrm{c}}(\boldsymbol{y}), \end{aligned} \tag{3}$$

where capital letters denote the macroscale fields assumed constant on Y, the subscript $\bullet_{\mathrm{c}}$ is used to denote correction fields assumed periodic on the cell Y and $\boldsymbol{y}$ represents the local coordinate vector in the cell. Periodicity relates to tangential components of $\boldsymbol{e}_c$ and $\boldsymbol{h}_c$ and to normal components of $\boldsymbol{b}_c$ and $\boldsymbol{j}_c$ on ∂Y. Here $\boldsymbol{J}$ is null as Y is insulated.

The mesoscale B-conforming formulation is derived using (1) and (3) as follow:

$$\operatorname{curl}\Big(\boldsymbol{\nu}\left(\boldsymbol{B} + \operatorname{curl}\boldsymbol{a}_c\right)\Big) + \boldsymbol{\sigma}\,\partial_t\Big(\boldsymbol{a}_c + \boldsymbol{B} \times \frac{\boldsymbol{y}}{d-1}\Big) = 0, \tag{4}$$

where the unknown potential $\boldsymbol{a}_c$ has a periodic tangential component across ∂Y, verifies $\boldsymbol{b}_c = \operatorname{curl}\boldsymbol{a}_c$ and has to be gauged in Y_{N}. The magnetic flux density, magnetic field strength and electric field are $\boldsymbol{b} = \boldsymbol{B} + \operatorname{curl}\boldsymbol{a}_c$, $\boldsymbol{h} = \boldsymbol{\nu}\boldsymbol{b}$ and $\boldsymbol{e} = -\partial_t \boldsymbol{a}_c - \partial_t \boldsymbol{B} \times \frac{\boldsymbol{y}}{d-1}$.

To define the macroscopic problem, let Ω_{H} be the homogenized domain replacing Ω^ϵ. The macroscopic vector potential $\boldsymbol{A}$ is the solution of (2b)-(2d) in $\Omega \setminus \Omega_{\mathrm{H}}$, but the equation in Ω_{H} must be defined for macroscopic fields. Since the current density is zero at macroscale, Ω_{H} is not conducting. Hence macroscopic Maxwell-Ampère's law reads

$$\operatorname{curl}\boldsymbol{H} = 0 \quad \text{ in } \Omega_{\mathrm{H}}, \tag{5}$$

where $\boldsymbol{H}$ is the upscaled magnetic field which will be computed from the mesoscale solution obtained by imposing the source $\boldsymbol{B}$ to the cell problem. In general, $\boldsymbol{H}$ is a nonlinear function of $\boldsymbol{B}$, and (5) can be solved iteratively, e.g. with :

$$\operatorname{curl}\left(\boldsymbol{H}(\boldsymbol{B}^k) + \left(\frac{\partial \boldsymbol{H}}{\partial \boldsymbol{B}}\right)^k (\boldsymbol{B}^{k+1} - \boldsymbol{B}^k)\right) = 0 \text{ in } \Omega_{\mathrm{H}}, \tag{6}$$

where $\boldsymbol{B}^{k+1} = \operatorname{curl}(\boldsymbol{A}^{k+1})$. The Jacobian $\frac{\partial \boldsymbol{H}}{\partial \boldsymbol{B}}^k$ can be computed using finite differences, its columns are given by:

$$\left(\frac{\partial \boldsymbol{H}}{\partial B_i}\right)^k = \frac{1}{\delta B}\Big(\boldsymbol{H}(\boldsymbol{B}^k + \delta B \boldsymbol{e}_i) - \boldsymbol{H}(\boldsymbol{B}^k)\Big) \text{ for } i = 1, \dots d,$$

where $\boldsymbol{e}_i$ are the standard basis vectors, δB is a scalar perturbation and k is the nonlinear iteration index. This Jacobian computation requires solving $d+1$ problems on each cell.

The definitions of macroscopic fields are needed to define the decomposition (3). The usual definition of macroscopic fields uses the volume average $<>_Y$ of the mesoscopic ones:

$$\boldsymbol{U} = <\boldsymbol{u}>_Y = \frac{1}{|Y|}\int_Y \boldsymbol{u} \quad \text{ for a field } \boldsymbol{u} \text{ on } Y,$$

where $|Y|$ is the volume of Y. This definition always works for $\boldsymbol{B}$ and $\boldsymbol{J}$, i.e.

$$\boldsymbol{B} = <\boldsymbol{b}>_Y, \quad \boldsymbol{J} = <\boldsymbol{j}>_Y, \tag{7}$$

because the surface average of the flux of $\boldsymbol{b}$ and $\boldsymbol{j}$ through the faces of ∂Y respectively sum up to volume average of $\boldsymbol{b}$ and $\boldsymbol{j}$ in Y (because $\operatorname{div}\boldsymbol{b} = 0$ and $\operatorname{div}\boldsymbol{j} = 0$), meaning that definition (7) is compatible with the continuity of $\boldsymbol{B}\cdot\boldsymbol{n}$ and $\boldsymbol{J}\cdot\boldsymbol{n}$ on $\partial\Omega_{\mathrm{H}}$. Combining (3) and (7) yields $< \boldsymbol{b}_c >_Y = 0$, which is verified in (4) because

$$\int_Y \boldsymbol{b}_c = \int_Y \operatorname{curl}\boldsymbol{a}_c = \oint_{\partial Y} \boldsymbol{a}_c \times \boldsymbol{n} = 0,$$

where the integral on ∂Y vanishes due to anti-periodicity of $\boldsymbol{a}_c \times \boldsymbol{n}$.

The magnetic field $\boldsymbol{h}$ can also be upscaled using $<\boldsymbol{h}>_Y$ when eddy currents in Y are weak or non existent. Indeed, some previous work could obtain correct results using $<\boldsymbol{h}>_Y$ for dynamical problems with eddy currents (see e.g. [1], [2] and [3]), although the upscaling of $\boldsymbol{h}$ cannot generally be done in this way, as will be shown later. The problem comes from the fact that eddy currents impact the average of $\boldsymbol{h}$ without impacting the average of $\boldsymbol{j}$, leading the macroscopic Maxwell-Ampère's law to be wrong.

III. Magnetic field upscaling

Although all the geometries and numerical tests presented in this paper are done with an insulated cell, the material of this section is derived in the general setting of a conducting cell, but still with the assumption that Y_{c} is simply connected. In this section, we demonstrate how to properly upscale $\boldsymbol{H}$ by removing the part of $\boldsymbol{h}$ that generates the local eddy currents in $\boldsymbol{j}$. More precisely, we define a potential $\boldsymbol{t}_0$ such that $\operatorname{curl}\boldsymbol{t}_0 = \boldsymbol{j}_e$ such that $\boldsymbol{j}_e$ are the local eddy currents, and such that $\boldsymbol{t}_0 = 0$ when there are no eddy currents ($\boldsymbol{j}_e = 0$). Then $\boldsymbol{H}$ can be defined as

$$\boldsymbol{H} = <\boldsymbol{h} - \boldsymbol{t}_0>_Y . \tag{8}$$

The rest of the current $\boldsymbol{j}_{\mathrm{M}} = \boldsymbol{j} - \boldsymbol{j}_e$ is the flow of the macroscopic current in the cell.

A. A setting to study currents in the cell

The splitting $\boldsymbol{j} = \boldsymbol{j}_e + \boldsymbol{j}_{\mathrm{M}}$ will be defined with a Helmholtz-Hodge decomposition (HHD) [6]-[7]. Let $\Gamma_c = \partial Y_{\mathrm{c}}$ be the boundary of the cell conducting domain, $\Gamma_{\mathrm{c}}^{\mathrm{out}} = \Gamma_c \cap \partial Y$ the boundary of Y through which the current can flow and $\Gamma_{\mathrm{c}}^{\mathrm{in}} = \Gamma_c \setminus \Gamma_{\mathrm{c}}^{\mathrm{out}}$ the interface between the conducting and non conducting domain in Y.

The current density verifies $\operatorname{div}\boldsymbol{j} = 0$, $(\boldsymbol{j}\cdot\boldsymbol{n})\boldsymbol{n}$ is periodic through $\Gamma_{\mathrm{c}}^{\mathrm{out}}$, and the current cannot flow to the nonconducting domain, i.e. $\boldsymbol{j}\cdot\boldsymbol{n}|_{\Gamma_{\mathrm{c}}^{\mathrm{in}}} = 0$. We denote the space for $\boldsymbol{j}$ by $\boldsymbol{H}_{0,\mathrm{in}}^{\#,\mathrm{out}}(\operatorname{div}; Y_{\mathrm{c}})$, where $_{0,\mathrm{in}}$ is the usual notation for null trace on $\Gamma_{\mathrm{c}}^{\mathrm{in}}$ and where $^{\#,\mathrm{out}}$ denotes the trace periodicity on $\Gamma_{\mathrm{c}}^{\mathrm{out}}$.

It is hard to study $\boldsymbol{j}$ in $\boldsymbol{H}_{0,\mathrm{in}}^{\#,\mathrm{out}}(\operatorname{div}; Y_{\mathrm{c}})$ because it has mixed boundary conditions, and neither $\Gamma_{\mathrm{c}}^{\mathrm{in}}$ nor $\Gamma_{\mathrm{c}}^{\mathrm{out}}$ are closed and simply connected when the cell is not insulated. We thus introduce a simpler equivalent setting.

Let $\mathcal{Y}_{\mathrm{c}}$ be the periodized Y_{c}, that is Y_{c} but with the opposite components of $\Gamma_{\mathrm{c}}^{\mathrm{out}}$ identified. The boundary $\partial\mathcal{Y}_{\mathrm{c}}$ is $\Gamma_{\mathrm{c}}^{\mathrm{in}}$ periodized, so that $\partial\mathcal{Y}_{\mathrm{c}}$ is a closed surface while $\Gamma_{\mathrm{c}}^{\mathrm{in}}$ is not. There is a natural one to one correspondence between fields

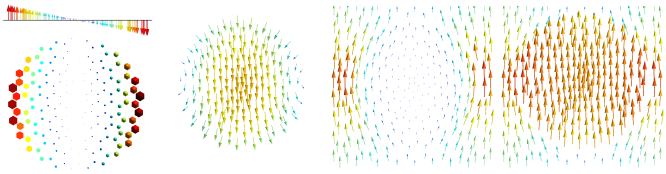

Fig. 1. Example of HHD in a 2D insulated conducting sphere at high frequency, from left to right : $\boldsymbol{j} = \boldsymbol{j}_e$ (two viewpoints), $\boldsymbol{t}_0$, $\boldsymbol{h}$ and $\boldsymbol{h} - \boldsymbol{t}_0$.

on $\mathcal{Y}_c$ and the fields on Y_c with periodic trace on Γ_c^{out}. In particular $\boldsymbol{H}^{\#,out}_{0,in}(\mathrm{div}; Y_c)$ is isomorphic to $\boldsymbol{H}_0(\mathrm{div}; \mathcal{Y}_c)$. We use symbols $\mathring{\boldsymbol{j}}$, $\mathring{\boldsymbol{t}}$ for the fields defined on $\mathcal{Y}_c$ corresponding to the Γ_c^{out}-periodic fields $\boldsymbol{j}$, $\boldsymbol{t}$ defined on Y_c.

B. Helmholtz-Hodge decomposition

In general, any vector field $\mathring{\boldsymbol{j}}$ on $\mathcal{Y}_c$ can be orthogonally decomposed as follows with a HHD (see eq. (7) from [7][1]):

$$\mathring{\boldsymbol{j}} = \mathrm{grad}\,\mathring{\phi} + \mathrm{curl}\,\mathring{\boldsymbol{t}}_0 + \mathring{\boldsymbol{j}}_t \quad \text{in } \mathcal{Y}_c \tag{9}$$

where $\mathring{\phi} \in H(\mathrm{grad}; \mathcal{Y}_c)$, $\mathring{\boldsymbol{t}}_0 \in \boldsymbol{H}_0(\mathrm{curl}; \mathcal{Y}_c)$ and $\mathring{\boldsymbol{j}}_t \in \boldsymbol{\mathcal{H}}^1(\mathcal{Y}_c)$ is a tangential harmonic field, i.e. it is curl- and divergence-free and $\mathring{\boldsymbol{j}}_t \cdot \boldsymbol{n}|_{\partial\mathcal{Y}_c} = 0$. $\boldsymbol{\mathcal{H}}^1(\mathcal{Y}_c)$ is the first co-homology space, its dimension β_1 is the finite number of loops that $\mathcal{Y}_c$ forms, and its elements (e.g. $\mathring{\boldsymbol{j}}_t$) are harmonic fields looping in its loops [7]. In addition, the flux of $\mathring{\boldsymbol{t}}_0$ through each connected component of $\partial\mathcal{Y}_c$ must be 0 to nullify its normal harmonic components.

The general decomposition (9) is simpler for $\mathring{\boldsymbol{j}}$ with

$$\mathrm{grad}\,\mathring{\phi} = 0 \text{ in } \mathcal{Y}_c. \tag{10}$$

Indeed, by definition, all three $\mathring{\boldsymbol{j}}$, $\mathring{\boldsymbol{j}}_t$ and $\mathrm{curl}\,\mathring{\boldsymbol{t}}_0$ are divergence free and tangential to $\partial\mathcal{Y}_c$. Applying the divergence operator on (9) yields $\mathrm{div}\,(\mathrm{grad}\,\mathring{\phi}) = 0$. Similarly, taking the trace of (9) yields $\mathrm{grad}\,\mathring{\phi} \cdot \boldsymbol{n}|_{\partial\mathcal{Y}_c} = 0$. Then

$$\begin{aligned}\|\mathrm{grad}\,\mathring{\phi}\|^2 &= \int_{\mathcal{Y}_c} \mathrm{grad}\,\mathring{\phi} \cdot \mathrm{grad}\,\mathring{\phi} \\ &= -\int_{\mathcal{Y}_c} \mathrm{div}(\mathrm{grad}\,\mathring{\phi})\,\mathring{\phi} + \int_{\partial\mathcal{Y}_c} (\mathrm{grad}\,\mathring{\phi} \cdot \boldsymbol{n})\,\mathring{\phi} = 0.\end{aligned}$$

At this point, we can define the decomposition of $\boldsymbol{j}$ on Y_c. Let $\boldsymbol{t}_0 \in \boldsymbol{H}^{\#,out}_{0,in}(\mathrm{curl}; Y_c)$ be the field corresponding to $\mathring{\boldsymbol{t}}_0$, $\boldsymbol{j}_M$ the one corresponding to $\mathring{\boldsymbol{j}}_t$ and define $\boldsymbol{j}_e = \mathrm{curl}\,\boldsymbol{t}_0$. We have the unique orthogonal decomposition

$$\boldsymbol{j} = \boldsymbol{j}_e + \boldsymbol{j}_M \text{ in } Y_c. \tag{11}$$

Moreover, the decomposition verifies

$$< \boldsymbol{j}_e >_{Y_c} = 0, \quad \text{and} \quad < \boldsymbol{j}_M >_Y = \boldsymbol{J} \tag{12}$$

$$(\boldsymbol{j}_e = 0 \implies < \boldsymbol{t}_0 >_Y = 0). \tag{13}$$

Proof of (12): $\int_{Y_c} \boldsymbol{j}_e = \int_{Y_c} \mathrm{curl}\,\boldsymbol{t}_0 = \int_{\partial Y_c} \boldsymbol{t}_0 \times \boldsymbol{n} = \int_{\Gamma_c^{in}} \boldsymbol{t}_0 \times \boldsymbol{n} + \int_{\Gamma_c^{out}} \boldsymbol{t}_0 \times \boldsymbol{n} = 0$ because both integrals vanish due to $\boldsymbol{t}_0 \times \boldsymbol{n}$ nullity on Γ_c^{in} and anti-periodicity on Γ_c^{out}. Then $< \boldsymbol{j}_M >_Y = < \boldsymbol{j} >_Y - < \boldsymbol{j}_e >_Y = < \boldsymbol{j} >_Y = \boldsymbol{J}$.

Proof of (13): when $\mathrm{curl}\,\mathring{\boldsymbol{t}}_0 = 0$ in $\mathcal{Y}_c$, there exist $\mathring{\psi}_0 \in H_0(\mathrm{grad}; \mathcal{Y}_c)$ such that $\mathring{\boldsymbol{t}}_0 = \mathrm{grad}\,\mathring{\psi}_0$ (because $\mathring{\boldsymbol{t}}_0$ contains no harmonic part). Now coming back in Y_c, one gets $\boldsymbol{t}_0 = \mathrm{grad}\,\psi_0$ where $\psi_0 \in \boldsymbol{H}^{\#,out}_{0,in}(\mathrm{grad}; Y_c)$. Finally,

$$\int_{Y_c} \boldsymbol{t}_0 = \int_{Y_c} \mathrm{grad}\,\psi_0 = \int_{\Gamma_c^{in}} \psi_0 \boldsymbol{n} + \int_{\Gamma_c^{out}} \psi_0 \boldsymbol{n} = 0,$$

where both integrals vanish due to the nullity of $\psi_0 \boldsymbol{n}$ on Γ_c^{in} and its anti-periodicity on Γ_c^{out}.

To sum up, the decomposition (11) is orthogonal and unique and its properties have a desirable physical meaning. The "macroscopic current flow" $\boldsymbol{j}_M$ flows through ∂Y, averages to $\boldsymbol{J}$ and has zero curl. On the other hand, the eddy currents $\boldsymbol{j}_e$ have zero average and contain all "curling" currents ($\mathrm{curl}\,\boldsymbol{j} = \mathrm{curl}\,\boldsymbol{j}_e$). The potential $\boldsymbol{t}_0$ is defined to represent the part of $\boldsymbol{h}$ that creates $\boldsymbol{j}_e$. Indeed $\mathrm{curl}\,(\boldsymbol{h} - \boldsymbol{t}_0) = \boldsymbol{j} - \boldsymbol{j}_e = \boldsymbol{j}_M$ and the average of $\boldsymbol{t}_0$ vanishes when eddy currents vanish (13).

C. Macroscopic magnetic field computation

As stated before (8), we propose to define the macroscopic field as $\boldsymbol{H} = < \boldsymbol{h} - \boldsymbol{t}_0 >_Y$. This way, the local currents $\boldsymbol{j}_e$ no longer impact $\boldsymbol{H}$, which is consistent with the macroscopic Maxwell-Ampère's law which relates to $\boldsymbol{J}$ but not $\boldsymbol{j}_e$.

The potential $\boldsymbol{t}_0$ can be extracted from $\boldsymbol{j}$ by solving the projection $\mathrm{curl}\,(\boldsymbol{j} - \mathrm{curl}\,\boldsymbol{t}_0) = 0$ in Y_c. When $\boldsymbol{j}$ is the solution of (4) and the cell is insulated, the FEM weak form reads:

$$\int_{Y_c} \boldsymbol{\sigma}\,\partial_t\left(\boldsymbol{a}_c + \boldsymbol{B} \times \frac{\boldsymbol{y}}{d-1}\right) \mathrm{curl}\,\boldsymbol{t}_0' + \int_{Y_c} \mathrm{curl}\,\boldsymbol{t}_0\,\mathrm{curl}\,\boldsymbol{t}_0' = 0 \tag{14}$$

for all $\boldsymbol{t}_0'$, with $\boldsymbol{t}_0, \boldsymbol{t}_0' \in \boldsymbol{H}_0(\mathrm{curl}; Y_c)$. Here the periodicity of $\boldsymbol{t}_0$ is not applied because $\Gamma_c^{out} = \emptyset$. And nothing is needed to ensure that $\boldsymbol{t}_0$ cannot contain a normal harmonic part, because Γ_c^{in} is connected. A decomposition example is shown Fig. 1.

Alternatively, when Y_c is insulated, it is possible to compute $\boldsymbol{H}$ in another way. Introducing $< \boldsymbol{u} >_{\partial Y_\parallel}$ the tangential average of a vector field $\boldsymbol{u}$ over ∂Y, it is defined by:

$$< \boldsymbol{u} >_{\partial Y_\parallel} = \sum_{i=x,y,z} \frac{1}{|\partial Y_i|} \int_{\partial Y_i} u_t, \tag{15}$$

where ∂Y_i are faces of ∂Y with normal $\boldsymbol{n} = \boldsymbol{e}_i$ and $\boldsymbol{u}_t = (\boldsymbol{n} \times \boldsymbol{u}) \times \boldsymbol{n}$. One can prove that $< \boldsymbol{u} >_{\partial Y_\parallel} = < \boldsymbol{u} >_Y$ whenever $\boldsymbol{u}_t$ is Y-periodic and $\mathrm{curl}\,\boldsymbol{u} = 0$ on Y. In an insulated cell, $\mathrm{curl}\,(\boldsymbol{h} - \boldsymbol{t}_0) = \boldsymbol{j}_M = 0$, thus

$$\boldsymbol{H} = < \boldsymbol{h} - \boldsymbol{t}_0 >_Y = < \boldsymbol{h} - \boldsymbol{t}_0 >_{\partial Y_\parallel} = < \boldsymbol{h} >_{\partial Y_\parallel}, \tag{16}$$

where the last equality is due to $\boldsymbol{t}_0|_{\partial Y} = 0$. So the simple boundary integration $< \boldsymbol{h} >_{\partial Y_\parallel}$ can be used to upscale $\boldsymbol{H}$ without doing the FEM computation of $\boldsymbol{t}_0$. But this alternative is only available for insulated cell, and might lead to more numerical error than using the volume average (8).

IV. Validation

The validation is done on a 2D insulated cell of width $100\,\mu$m with a conducting disks of radius $40\,\mu$m (see Fig. 4). If not mentioned otherwise, we consider $f = 100$ MHz, $\boldsymbol{\nu} = \boldsymbol{\nu}_0$ everywhere, $\boldsymbol{\sigma} = 1.01 \times 10^7$ S/m in the disk and $\boldsymbol{\sigma} = 0$ outside.

[1]The correspondence between [7] notations and ours is : $\mathcal{Y}_c = \mathcal{M}$, $\partial\mathcal{Y}_c = \partial\mathcal{M}$, $\mathring{\boldsymbol{j}} = \omega^2$, $\mathring{\boldsymbol{t}}_0 = \alpha_n^1$, $\mathring{\boldsymbol{j}}_t = h_n^2$, curl $= d^1$ and $-$grad $= \delta^3$. As h_t^2 and η^2 can both be written as codifferential δ^3, we merged them with $\delta^3\beta_t^3$ in our grad $\mathring{\phi}$ term. The decomposition (9) is still orthogonal in 2D because h_n and $h_t + \eta$ are always orthogonal (see comments about Friedrichs decomposition).

A. Tests on a single cell problem

A first validation is done using the H-conforming formulation of the cell problem with the imposed source $\boldsymbol{H}(t)$ known at every time step t. Figure 2 shows the validation that the proposed methods work, unlike the volume average.

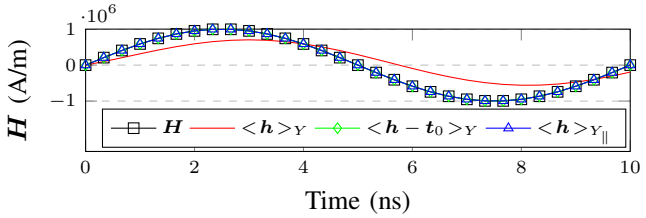

Fig. 2. Comparison of the magnetic field upscaling strategies, over one period of $\boldsymbol{H}$, which is sinusoidal. The proposed methods $<\boldsymbol{h}-\boldsymbol{t}_0>_Y$ (8) and $<\boldsymbol{h}>_{Y_\parallel}$ (16) match $\boldsymbol{H}$, but the volume average $<\boldsymbol{h}>_Y$ doesn't.

To explain why previous use of $<\boldsymbol{h}>_Y$ as the upscaling formula were successful, the plots on Fig. 3 show that the error committed is correlated with the percentage of the Joule losses in the total electromagnetic power of the cell. This percentage depends on the physical parameters, geometry, and especially on the frequency. Using $\boldsymbol{H} = <\boldsymbol{h}>_Y$ below $f = 500$ kHz would work fine to stay below 1% of error. In general, simulation of magnetic cores with small Joule losses are unlikely to require our approach.

B. Multiscale model validation

A full 2D multiscale problem is solved with FEM B-conforming formulation at macro and meso scales. The studied periodic geometry Ω^ϵ is a square of 10 by 10 cells. A source field is generated by an external inductor coil surrounding Ω^ϵ and fed by a sinusoidal current. The coil has a radius of $40\,\mu$m and is $670\,\mu$m away from Ω^ϵ (Fig. 4 top).

Heterogeneous Multiscale Method (HMM) [3] is used for the multiscale problem, i.e. a cell problem is associated to each element of the macro mesh, which do not have to correspond to the real geometry tiling. The macro and meso problems are solved alternatively. The reference mesh takes into account the real geometry of Ω^ϵ. Problems are meshed with Gmsh [8] and solved using GetDP [9].

Using $<\boldsymbol{h}>_{\partial Y_\parallel}$, HMM yields the correct value of the total Joule losses over one period with 1.34% of error compared to the reference, versus 90.2% with $<\boldsymbol{h}>_Y$ (Fig. 5).

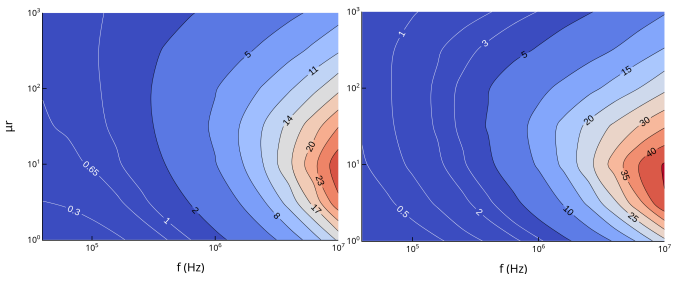

Fig. 3. Log-log error contour maps in the meso cell exited by a sinusoidal $\boldsymbol{B}$ source, at different frequencies and at different sphere relative permeabilities. Left : percentage of difference between $\int_0^T \|H(t) - <h(t)>_Y\| dt$ and $\int_0^T \|<h(t)>_Y\| dt$. Right : percentage of the Joule losses power percentage in the total electromagnetic power.

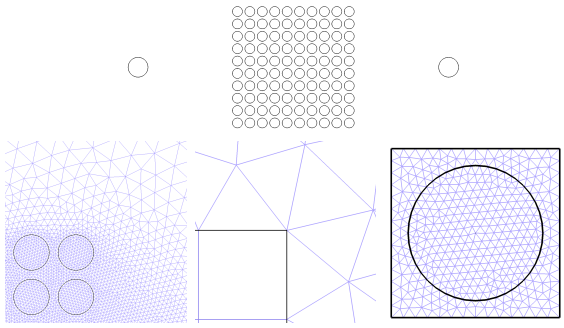

Fig. 4. Geometry for multiscale test with the two inductor cuts on the sides (top), meshes of corners of Ω^ϵ and Ω_H (left & middle), one cell mesh (right).

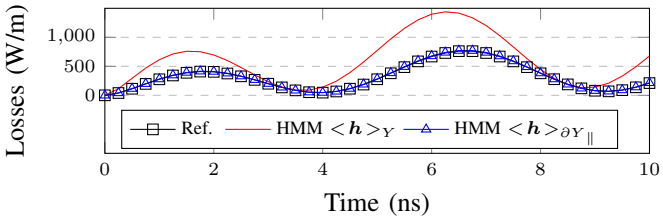

Fig. 5. Joule losses power comparison in the multiscale simulation.

V. Conclusion

This paper presented the ins and outs of magnetic field homogenization on geometries with insulated periodic cells. Firstly by demonstrating the limitation of the volume average and its dependency on the eddy currents power ratio in the total electromagnetic power. Secondly by proposing a general definition of the homogenized magnetic field which is mathematically well defined and comprehensive with physical insights. And finally by validating the proposed definitions on multiscale solutions.

As future perspectives, the method should be validated on a 3D geometry, and with nonzero macroscopic current. It can also be extended to geometries with multi-connected cell conducting domains. Finally, the same approach could be used for the electric field upscaling.

References

[1] M. El Feddi, Z. Ren, A. Razek, A. Bossavit, "Homogenization technique for Maxwell equations in periodic structures" IEEE Transactions on Magnetics, 1997.

[2] O. Bottauscio, V. Chiadò Piat, M. Chiampi, M. Codegone, A. Manzin, "Nonlinear Homogenization Technique for Saturable Soft Magnetic Composites" IEEE Transactions on Magnetics, 2008.

[3] I, Niyonzima, R.V. Sabariego, P. Dular, C. Geuzaine, "Nonlinear Computational Homogenization Method for the Evaluation of Eddy Currents in Soft Magnetic Composites" IEEE Transactions on Magnetics, 2014.

[4] G. Meunier, V. Charmoille, C. Guerin, P. Labie and Y. Marechal, "Homogenization for Periodical Electromagnetic Structure: Which Formulation?" IEEE Transactions on Magnetics, 2010.

[5] A. Kameari, "Calculation of Transient 3D Eddy Current Using Edge-Elements." IEEE Transactions on Magnetics 26, 1990.

[6] H. Bhatia, G. Norgard, V. Pascucci, P.T. Bremer, "The Helmholtz-Hodge Decomposition—A Survey" IEEE Transactions on Visualization and Computer Graphics, 2013.

[7] Z. Rundong, M. Desbrun, G.W. Wei, Y. Tong, "3D Hodge Decompositions of Edge- and Face-Based Vector Fields". ACM Transactions on Graphics 38, 2019.

[8] C. Geuzaine, J.F. Remacle; Gmsh: https://gmsh.info

[9] P. Dular, C. Geuzaine; GetDP: https://getdp.info